The Journal of Physiology



# Scale-invariant changes in corticospinal excitability reflect multiplexed oscillations in the motor output

Marco Emanuele[1,2,3], Alessandro D'Ausilio[1,2], Giacomo Koch[1,4], Luciano Fadiga[1,2] and Alice Tomassini[2]

[1]*Department of Neuroscience and Rehabilitation, Section of Physiology, University of Ferrara, Ferrara, Italy*
[2]*Center for Translational Neurophysiology of Speech and Communication, Istituto Italiano di Tecnologia, Ferrara, Italy*
[3]*Department of Computer Science, Western University, London, Ontario, Canada*
[4]*IRCSS Santa Lucia, Roma, Italy*

Handling Editors: Richard Carson & James Coxon

The peer review history is available in the Supporting Information section of this article (https://doi.org/10.1113/JP284273#support-information-section).

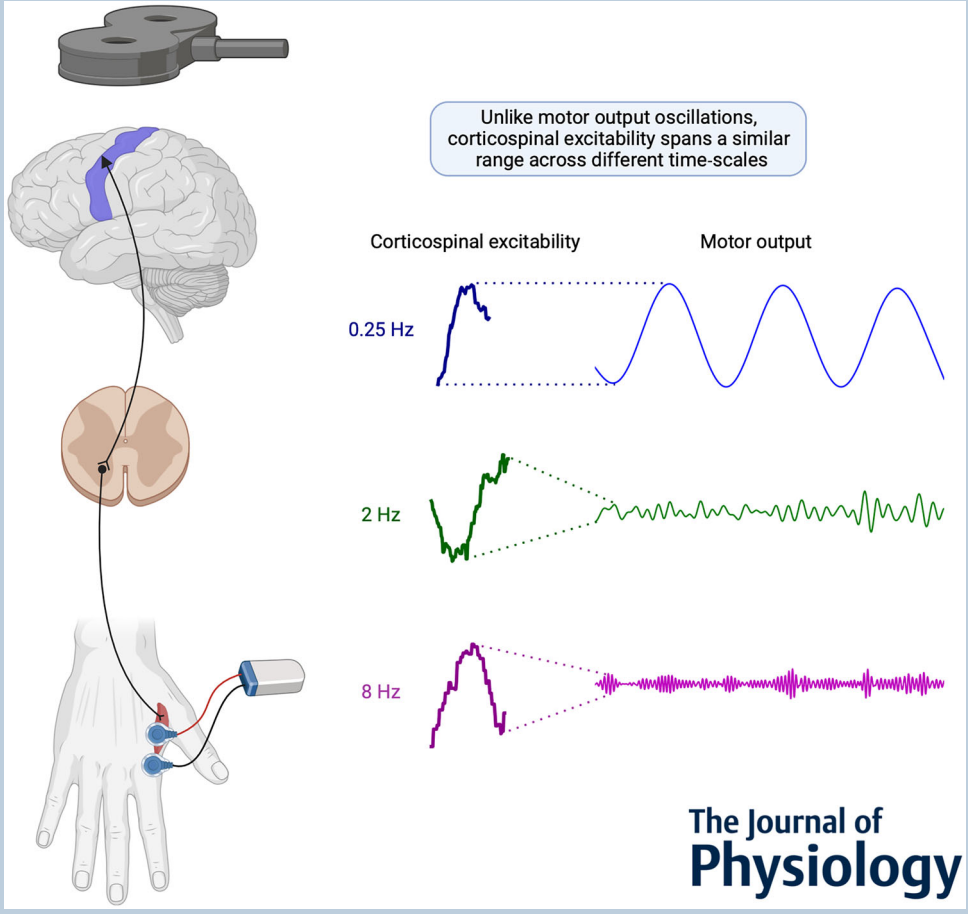


**Abstract** In the absence of disease, humans produce smooth and accurate movement trajectories. Despite such 'macroscopic' aspect, the 'microscopic' structure of movements reveals recurrent (quasi-rhythmic) discontinuities. To date, it is unclear how the sensorimotor system contributes

L. Fadiga and A. Tomassini are joint last authors.



DOI: 10.1113/JP284273

to the macroscopic and microscopic architecture of movement. Here, we investigated how corticospinal excitability changes in relation to microscopic fluctuations that are naturally embedded within larger macroscopic variations in motor output. Participants performed a visuomotor tracking task. In addition to the 0.25 Hz modulation that is required for task fulfilment (macroscopic scale), the motor output shows tiny but systematic fluctuations at ∼2 and 8 Hz (microscopic scales). We show that motor-evoked potentials (MEPs) elicited by transcranial magnetic stimulation (TMS) during task performance are consistently modulated at all (time) scales. Surprisingly, MEP modulation covers a similar range at both micro- and macroscopic scales, even though the motor output differs by several orders of magnitude. Thus, corticospinal excitability finely maps the multiscale temporal patterning of the motor output, but it does so according to a principle of scale invariance. These results suggest that corticospinal excitability indexes a relatively abstract level of movement encoding that may reflect the hierarchical organisation of sensorimotor processes.

(Received 16 December 2022; accepted after revision 22 November 2023; first published online 7 December 2023)
**Corresponding authors** M. Emanuele and A. Tomassini: Department of Neuroscience and Rehabilitation, Section of Physiology, University of Ferrara, Ferrara, Italy. Email: mnlmrc@unife.it and alice.tomassini@iit.it

**Abstract figure legend** Corticospinal excitability shows modulations locked to motor output fluctuations on multiple timescales, namely the task-instructed pace (0.25 Hz), submovements (2 Hz) and physiological tremor (8 Hz). Yet, this modulation does not scale with the amplitude of motor output fluctuations, but obeys a principle of scale invariance. In fact, while the amplitude of motor output varies by orders of magnitude across (time)scales, corticospinal excitability spans a comparable range. Therefore, corticospinal excitability indexes a relatively abstract level of movement encoding that could leverage scale invariance principles to optimise sensorimotor processes by preserving similar control resolution across scales.

**Key points**

- Motor behaviour is organised on multiple (time)scales.
- Small but systematic ('microscopic') fluctuations are engrained in larger and slower ('macroscopic') variations in motor output, which are instrumental in deploying the desired motor plan.
- Corticospinal excitability is modulated in relation to motor fluctuations on both macroscopic and microscopic (time)scales.
- Corticospinal excitability obeys a principle of scale invariance, that is, it is modulated similarly at all (time)scales, possibly reflecting hierarchical mechanisms that optimise motor encoding.

## Introduction

Voluntary movements rely on neural control signals that operate on multiple timescales. The inherent multiscale nature of motor control is mirrored by the anatomo-functional architecture of the motor circuits. In fact, neural signals cycle across cortico-subcortical sensorimotor loops nested within one another, reaching spinal centres through several descending systems. These include direct pathways travelling along the pyramidal tract and forming mono- and oligo-synaptic connections with spinal targets (Bernhard et al., 1953; Kuypers, 1964; Lemon, 2008) and indirect projections that are relayed by subcortical structures, such as the reticular formation

**Marco Emanuele** is currently a Postdoctoral Research Associate at the University of Western Ontario, London, Canada. His research addresses the principles that govern motor control in healthy humans, and their alterations in clinical populations (e.g. children with autism, adult patients with movement disorders). Working in parallel along these two lines of research, he aims to investigate how movements are regulated in absence of disease and to exploit this knowledge to understand motor control alterations in clinical populations. Specifically, among the topics he has investigated are motor synergies, multiscale motor control, and sensorimotor integration.

(Fregosi et al., 2017; Keizer & Kuypers, 1989; Kuypers, 1964; Lemon, 2008). Eventually, descending signals are all channelled through one common final pathway, the $\alpha$-motoneuron, before being dispatched to the muscles (Sherrington, 1904).

It is remarkable how such a complex architecture results in smooth and accurate movement trajectories. Although mostly concealed from view, part of the multiscale organisation of motor control becomes apparent by zooming into the microstructure of movements. Microscopic fluctuations are often embedded, and mostly covered up, within larger macroscopic variations in force/kinematics. Interestingly, these small fluctuations in motor output are neither erratic nor sparse; force (and movement velocity) typically shows periodicity in two main frequency ranges, that is, approximately 2 and 8 Hz. The first component at 2 Hz is generally referred to as movement intermittency (or submovements) (Craik, 1947; Miall et al., 1986, 1993; Woodworth, 1899), while the second component at 8 Hz is related to physiological tremor (Elble, 1996; Horsley & Schäfer, 1886; Marshall & Walsh, 1956; McAuley & Marsden, 2000; Vallbo & Wessberg, 1993).

Here, we investigated the contribution of the corticospinal system in shaping the temporal structure of the motor output across macro- and microscopic scales. Differently from prior evidence based on measures of brain–muscle (as well as force/kinematics) coupling (e.g. Jerbi et al., 2007; Williams et al., 2009), in this study we measured electromyographic (EMG) responses, known as motor evoked potentials (MEPs), to single-pulse transcranial magnetic stimulation (TMS) over the primary motor cortex (M1). TMS generates brief volleys of neural activity that are transmitted trans-synaptically to corticospinal neurons, thus propagating downstream to $\alpha$-motoneurons (Di Lazzaro et al., 2008) and eliciting MEPs in the target muscle(s). MEPs offer a direct and instantaneous readout of the excitability of the corticospinal system at the time of stimulation (Rothwell, 1997). Given that the corticospinal function is fundamental for dexterous hand movements (Lemon, 2008), we asked the participants to perform a motor task requiring fine finger control. We applied TMS at random times during continuous task performance and examined whether corticospinal excitability varies in relation to multiscale fluctuations in motor output.

## Methods

### Participants

Fourteen healthy participants (7 females; mean age: 23.5, SD: 2.03) volunteered for the study. They were naïve about the goals of the study and were paid (30 €) for their participation. All participants were right-handed (by self-report), with normal or corrected-to-normal vision, and reported no contraindications to TMS (Rossi et al., 2009). The study was designed and conducted in accordance with the *Declaration of Helsinki* and the guidelines of the local ethics committee (Comitato Etico di Area Vasta Emilia Centro, ref: EM255-2020_UniFe/170 592). All participants provided written informed consent before participating in the study.

### Experimental task and procedures

Participants were comfortably seated ∼60 cm in front of an LCD monitor (24-inch,120 Hz; VIEWPixx/EEG; VPixx Technologies Inc., Saint-Bruno, Canada) and kept both arms leaning forward on a support with their hands pronated. The experimental task required them to perform isometric bimanual abduction of the index fingers against two force sensors (six-axis force/torque transducers; F/T Sensor Gamma; ATI Industrial Automation, Rochester Hills, MI, USA) to control the 2D position of a cursor (green circle, radius: 0.04°) and track a target (red circle, same size of the cursor) moving along a circular path (radius: 4°; highlighted by a thick grey line) at a constant pace of 0.25 Hz (Fig. 1*A*; adapted from Susilaradeya et al., 2019). The 2D position of the cursor resulted from the vectorial sum of the forces exerted by the two fingers (mapped onto two orthogonal axes; see Fig. 1*A*). Because of the orthogonal orientation of the two force vectors, the index fingers were required to apply force sinusoidally at the same frequency as the target rotation frequency (i.e. 0.25 Hz) with a relative phase shift equal to $\pi/2$ (see Fig. 1*A*,*B*). Hereinafter, we denote the 0.25 Hz periodicity (4 s period) as the macroscopic scale, that is, the task-instructed variation in force. The target direction of rotation (clockwise or counterclockwise) and starting position (0°, 45°, 90°, 135°, 180°, 225°, 270° or 315°) were randomised across trials. The force produced by both fingers was acquired at 120 Hz using a Measurement Computing USB-1608GX board (Measurement Computing Corporation, Norton, MA, USA) and synchronised with the visual display using the built-in VIEWPixx TTL triggering system. Force data acquisition and real-time display of the cursor and target were controlled via MATLAB (The MathWorks, Inc., Natick, MA, USA) and the Psychophysics Toolbox extensions (Brainard, 1997; Pelli, 1997; Scheuer et al., 2007).

The participants were invited to the laboratory on two consecutive days. On the first day, they underwent a practice session in which they were allowed to familiarize themselves with the task until they could perform it without excessive fatigue and with reasonably good and stable tracking performance. The following

day, participants underwent the TMS experiment, which included 200 trials. The trial structure was identical for the practice session and the TMS experiment, except that no TMS pulses were delivered during the practice session. At the beginning of each trial, the red target was presented at its starting position (randomised; see above) for a random time interval ranging between 0.5 and 1.5 s. Then, the green cursor was presented, and participants were allowed 3 s to position the cursor on the target. At the end of this 3 s period, the target motion began and continued for 12 s (i.e. three cycles). In the TMS experiment, magnetic pulses were delivered in each trial (one pulse per trial) at random times ranging from 2 s to 10 s after the onset of the target motion (Fig. 1*B*).

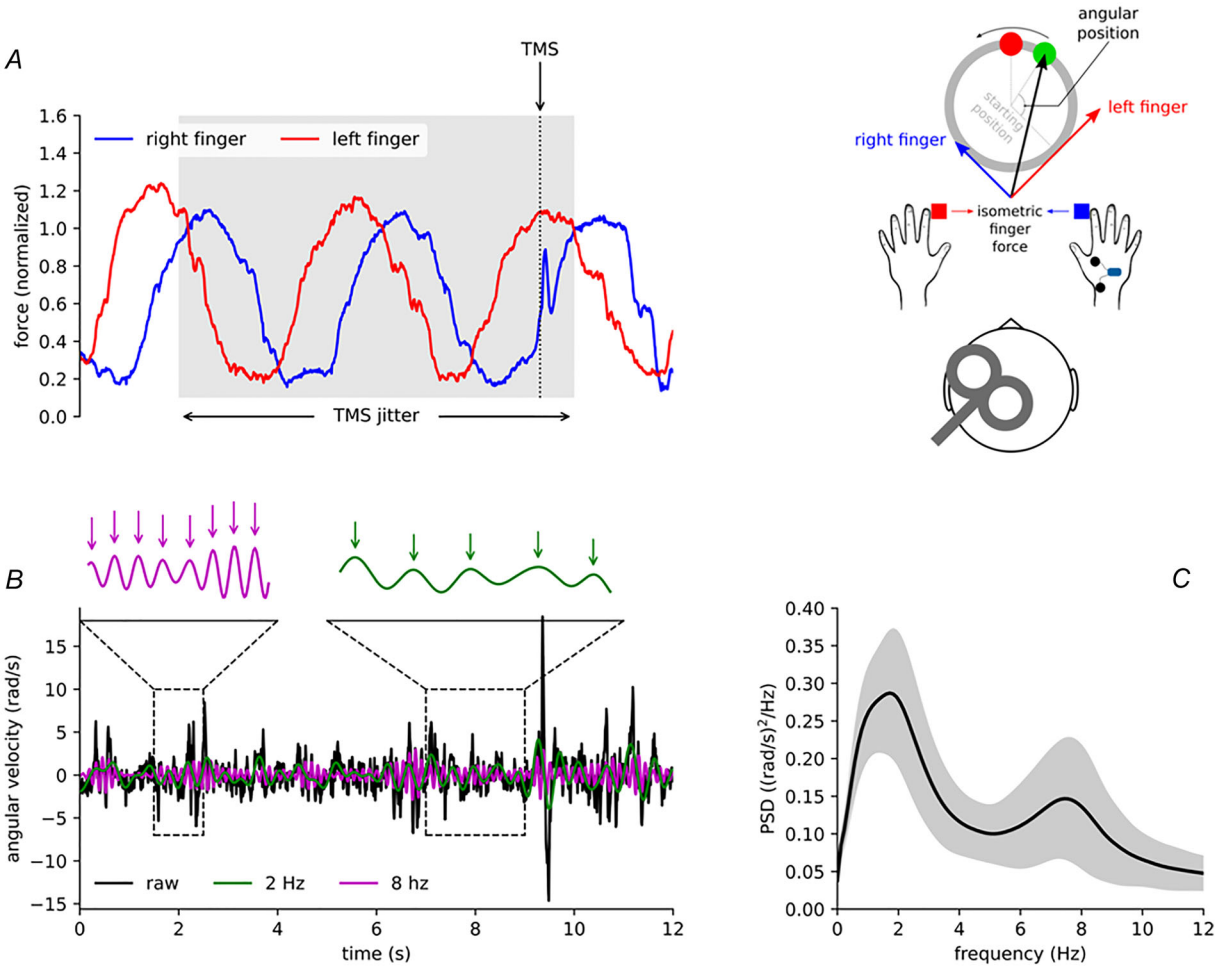


**Figure 1. Experimental task and procedure**
*A*, schematic representation of the visuo-motor tracking task (adapted from Susilaradeya et al., 2019) performed in combination with single-pulse TMS. Right panel, the participants controlled a cursor (green circle) to track a target (red circle) that moved along a circular path with a constant rotation frequency of 0.25 Hz. To control the cursor position, the participants exerted bimanual isometric abduction of the index finger against two force sensors. The forces applied by the right and left index fingers were mapped onto two orthogonal vectors pointing upward–leftward and upward–rightward, respectively. TMS was delivered to the left M1, and MEPs were recorded from the right FDI. Left panel, force produced by the right and left fingers in an example trial (normalised to the maximal nominal force; see Methods). By task design, the force varies sinusoidally at ∼0.25 Hz – the target rotation frequency – with a phase shift of $\pi/2$ between the two fingers. The dashed vertical line indicates the time when the TMS pulse was delivered in the example trial; the area highlighted in grey indicates the (across-trials) temporal jitter of the TMS pulse (i.e. 8 s). *B*, the black line shows the angular velocity of the cursor for the same example trial as shown in *A*; submovements (green) and tremor (violet) are highlighted by band-pass filtering of the velocity time series in the relevant frequency ranges (0.5–3 Hz and 6–10 Hz, respectively; see Methods). *C*, power spectral density (PSD) of the cursor angular velocity averaged across trials and participants. The shaded area represents the mean ± standard deviation. [Colour figure can be viewed at wileyonlinelibrary.com]

## TMS and EMG recordings

EMG was recorded from the right and left first dorsal interosseous (FDI) muscle (acting as the prime mover muscle in the current task; EMG data from the left finger were not analysed) using Ag–AgCl surface electrodes positioned according to a tendon–belly montage. The skin was carefully cleaned with alcohol before positioning the electrodes to improve the impedance. EMG was recorded with a wireless system (Wave Plus wireless EMG system; Cometa srl, Bareggio, Italy) and acquired at 5000 Hz using a CED board (Micro1401 mk II; Cambridge Electronic Design, Cambridge, UK). EMG data acquisition was synchronised with visual display (and force acquisition) using the TTL triggering system of the VIEWPixx monitor. TMS was delivered to the left M1 using a 70 mm figure-of-eight coil connected to a Magstim 200 stimulator (The Magstim Company, Ltd, Whitland, UK). The coil was held tangentially to the scalp, with the handle pointing downward and backward, and oriented ∼45° away from the midline. The stimulation site on the scalp corresponds to the cortical representation of the FDI muscle. To set the stimulator intensity, we asked participants to apply sufficient force with their fingers to maintain the cursor at 45° along the circular trajectory. In this position, the force level exerted by the right index finger was halfway between the minimum and maximum required in the task. The stimulation intensity was tuned (participant-wise) to elicit ∼1 mV MEPs in this condition. This allowed the elicitation of detectable MEPs throughout the whole 0.25 Hz force cycle and, at the same time, avoided MEP saturation at the highest force levels (possibly concealing modulations induced by experimental manipulations).

## Data analysis

Data analysis was performed using custom-made Python code. The peak-to-peak MEP size was calculated in each trial and standardised ($z$-score normalisation: zero mean, unit variance) within each participant. The force was normalised to the nominal maximum required for the task. The EMG activity was high-pass filtered at 30 Hz (zero-phase FIR filter; kernel length: four cycles), rectified and finally $z$-scored for each participant. All filters were designed and applied using the 'firwin' and 'filtfilt' function of the SciPy library (Virtanen et al., 2020), respectively.

**Macroscopic scale.** We first assessed whether corticospinal excitability, as indexed by MEPs, varies according to the force produced (by the right finger) at the macroscopic scale (i.e. 0.25 Hz; task-instructed rate), consistent with previously reported findings (Hess et al., 1986). To this end, the force produced by the right index finger was low-pass filtered at 0.5 Hz (zero-phase FIR filter; kernel length: four cycles), and all the peaks (local maxima) in the signal were identified. We then time-aligned all data (force, EMG and MEPs) to the identified peaks. Specifically, for MEP data, we calculated TMS latency relative to the closest preceding peak in the force. MEPs were then binned (bin size: 1 s; overlap: 96%). Note that due to the large overlap among bins, each MEP contributes to several adjacent time-bins. The choice of binning parameters (bin size, overlap) influences the graphical representation of the time course of corticospinal excitability time-locked to force (and velocity, see below) fluctuations (e.g. see Fig. 3*C*) but does not affect the linear regression analysis used for the statistical evaluation of MEP modulation (see below). Furthermore, we compared the mean corticospinal excitability and EMG activity during the ramp-up and ramp-down phases of the force cycle to assess their hysteretic behaviour with respect to the produced force. For each participant, MEPs were assigned to one or other phase of the cycle based on the positive/negative sign of the instantaneous derivative of the right finger force (low-pass filtered) at the time of the TMS pulse.

**Microscopic scales.** The slow sinusoidal variation in the force produced by the finger(s) is not smooth but contains faster and smaller fluctuations (see Fig. 1). In the force traces, these faster components are largely obscured by the macroscopic modulation (see Fig. 1*A*, where force traces are dominated by the slow 0.25 Hz modulation and microscopic oscillations are barely visible). However, thanks to the bimanual nature of the task, the combined motor output from the right and left fingers (vector sum) can be translated into the cursor angular position. Its derivative (i.e. angular velocity) has, by task instructions, a constant value (on average), and therefore it shows no systematic fluctuation at 0.25 Hz (see Fig. 1*A* and *B* and Fig. 2). When analysed in the frequency domain, the cursor velocity yields only two distinctive spectral peaks centred at approximately 2 and 8 Hz (Fig. 1*C*; Welch's method). These components fall within the frequency bands commonly associated with submovements (2 Hz) and tremor (8 Hz) (Miall et al., 1993; Vallbo & Wessberg, 1993). To determine whether MEPs were also modulated according to these smaller and faster oscillations in motor output, we first band-pass filtered the velocity signal within the relevant frequency ranges (between 0.5 and 3 Hz, and between 6 and 10 Hz, respectively, as determined by inspection of the power spectral density; zero-phase FIR filters, kernel length: four cycles 4*A*), and then localised the 2 and 8 Hz velocity peaks (local maxima) in the filtered signal. Similar to the analysis performed at the macroscopic scale, we then time-aligned all the data (velocity, force, EMG and MEPs) to the identified peaks. Note that band-pass filtering was only

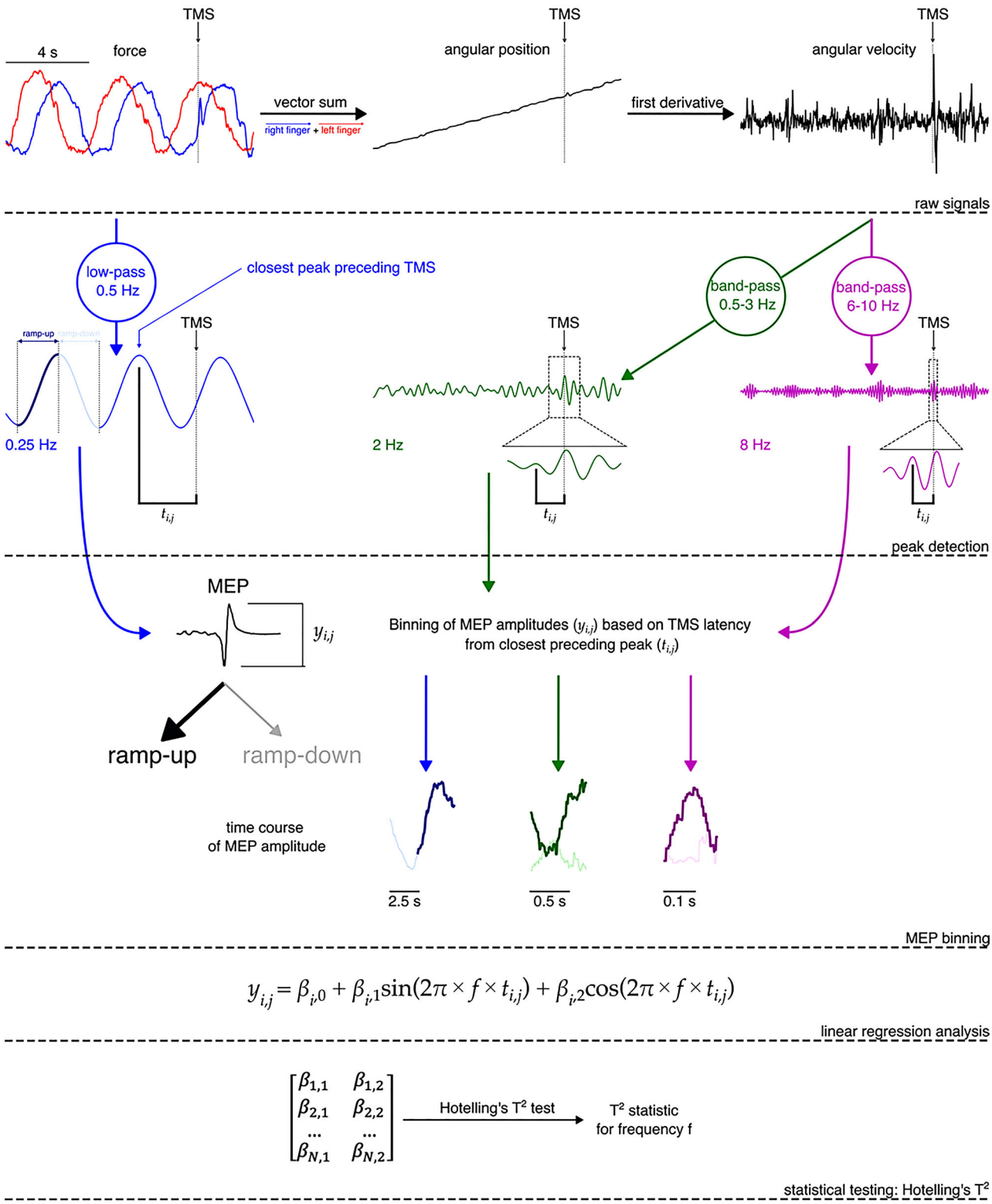


**Figure 2. Schematic of data analysis**
Example trial in which the TMS pulse was delivered in the ramp-up phase of the macroscopic force cycle. The same analysis pipeline shown here was applied also to ramp-down trials (i.e. trials in which the TMS pulse was delivered in the ramp-down phase of the macroscopic force cycle). [Colour figure can be viewed at wileyonlinelibrary.com]

used to identify the putative peaks in the velocity signal; data that were then time-locked to the identified peaks – i.e. force and EMG activity – were high-pass filtered (0.5 Hz) to remove the macroscopic modulation (Fig. 4*A*, second and third rows). MEPs were binned based on TMS latency relative to the closest preceding 2/8 Hz velocity peak. Data binning was tailored to each time-scale: for the 2 Hz time-scale, we binned the data for latencies ranging from 0.06 to 0.5 s (bin size: 0.12 s; overlap: 96%); for the 8 Hz time-scale, we binned the data over a correspondingly shorter time course ranging from 0.015 to 0.12 s (bin size: 0.03 s; overlap: 96%). As shown in Fig. 4*A* (first to third rows), peaks in the angular velocity can be easily traced back to the underlying right/left-finger force (and EMG) oscillations depending on the phase of the macroscopic force cycle in which they occur: when the force is increasing (ramp-up), FDI contraction produces a corresponding increase in the cursor velocity; conversely, when the force is decreasing (ramp-down), velocity peaks are associated with FDI relaxation. To account for this peculiar force-to-angular velocity mapping, MEPs elicited during the ramp-up and ramp-down phases of the 0.25 Hz cycle were analysed separately.

**Relationship between corticospinal excitability and motor output.** Previous work (De Noordhout et al., 1992; Hess et al., 1986, 1987) makes the expectation that, at each time-scale, MEPs scale with the instantaneous motor output at the time of TMS pulse delivery. To ascertain this, we first binned the EMG activity (rectified; unfiltered and filtered (0.5 Hz high-pass) for the macro- and microscopic scales, respectively) in the same way as performed for MEP data (i.e. as a function of time relative to the closest preceding force/velocity peak; see Methods, and Figs 2 and 3*A*). For each participant, we estimated the conduction delay along the corticospinal tract as the mean MEP latency (i.e. the time interval between the TMS pulse and MEP onset), calculated (trial-wise) as the earliest time point after the TMS pulse when the rectified EMG exceeded the baseline by at least 3 SDs (dispersion and mean used as baseline were computed within a 100 ms window before the TMS pulse). To quantify the relationship between corticospinal excitability and motor output, we then computed Pearson's correlation coefficient between MEP size and EMG activity (binned data), after time-shifting the latter by the estimated conduction delay (participant-wise).

We then studied how corticospinal excitability and motor output modulation varies in amplitude across different time-scales. We quantified the MEP modulation amplitude as the max − min difference in MEP size for data time-aligned to force/velocity peaks, separately for each participant, time-scale and phase of the force cycle (ramp-up/down) (Fig. 6*A*). The amplitude of oscillations in motor output – both force and EMG – were also estimated separately for each participant, time-scale and phase of the force cycle. To this end, force/EMG signals (unfiltered and 0.5 Hz high-pass filtered for the macro- and microscopic scales, respectively) were time-aligned to force/velocity peaks in the relevant time-scale and averaged (see above and Fig. 3*A* and *B* and Fig. 4*A*). The oscillation amplitude was calculated as the peak–trough difference over a time window (centred on force/velocity peaks) corresponding to about half a period at 0.25 Hz and one period at the microscopic scales. Therefore, at 0.25 Hz, we considered a 2 s window (0–2 s for ramp-down data; 2–4 s for ramp-up data; see Fig. 3); at 2 Hz, a 0.5 s window (from −0.25 to 0.25 s; see Fig. 4*A*, second row, left); and at 8 Hz, a 0.12 s window (from −0.06 to 0.06 s; see Fig. 4*A*, second row, right).

## Statistical analysis

Force, EMG activity and MEPs time-aligned to the 0.25 Hz force fluctuations (macroscopic scale) were compared between the ramp-up and ramp-down phases of the force cycle using paired sample Student's *t* test (Fig. 3).

To evaluate the consistency of the temporal modulation of corticospinal excitability across time-scales, we used an approach based on linear regression (similar to that used by Tomassini et al., 2017). For each trial, we computed the phase of a sinusoidal function as $2\pi \times f \times t$, where $f$ is the frequency (40 $\log_{10}$-spaced frequencies from 0.1 to 20 Hz) and $t$ is the TMS latency (relative to velocity/force peaks at each time-scale; see below for further details). The sine and cosine of this phase value were used (participant-wise) as predictors in a linear regression analysis, including the MEP as the dependent variable. The model behind the linear regression can be formalised as follows:

$$y_{i,j} = \beta_{i,0} + \beta_{i,1} \sin\left(2\pi \times f \times t_{i,j}\right) + \beta_{i,2} \cos\left(2\pi \times f \times t_{i,j}\right)$$

where $y_{i,j}$ and $t_{i,j}$ are the MEP and TMS latency of the $i$-th participant for the $j$-th trial, and $\beta_{i,0}$, $\beta_{i,1}$ and $\beta_{i,2}$ are the coefficients of the regression analysis for the $i$-th participant. We then tested whether the average of the participant-specific $\beta$-coefficients ($\beta_1$ and $\beta_2$) is significantly different from zero using the bivariate Hotelling's $T^2$ test. In practice, this corresponds to testing whether the MEP (time-aligned to 0.25 Hz force fluctuations or 2/8 Hz velocity peaks) is predicted by a sinusoidal function with the same frequency and phase across the participants. The resulting *P*-values were corrected for multiple comparisons across frequencies using the Bonferroni method. At the microscopic time-scales, we repeated the same analysis described above for angular velocity calculating the TMS latencies with respect to the peaks of tangential velocity (i.e.

the product of angular velocity of cursor trajectory radius) and the first derivative of the left and right finger forces (i.e. the velocity in the two orthogonal directions of motion controlled independently by the two hands); peaks were always detected after band-pass filtering of the signals within the relevant frequency ranges (2 Hz scale: 0.5–3 Hz, 8 Hz scale: 6–10 Hz; as described above). In contrast to velocity, the analysis performed on force (first derivative) did not require separation of the data according to the macroscopic force cycle (ramp-up/down). Linear regression analysis and statistical evaluation for left and right force were limited to the frequency intervals that were found to be statistically significant for angular velocity (see Results).

Correlation coefficients calculated at each time-scale between MEP size and EMG activity (binned data) were tested against zero by means of one-sample *t* tests.

Changes across time-scales of MEP modulation amplitude and amplitude of force and EMG oscillations were assessed by performing, separately for ramp-up and ramp-down data, a one-way ANOVA for repeated measures with 'Timescale' (0.25, 2 and 8 Hz) as a within-participant factor. Bonferroni-corrected paired sample *t* tests were used to assess pairwise comparisons. The non-significant results obtained with the traditional (i.e. 'frequentist') ANOVA were further explored with Bayesian statistics. In the presence of a negative result using frequentist statistics, the Bayesian approach allows the disentangling of 'absence of evidence [of a certain effect] from evidence of absence' (Keysers et al., 2020). Bayesian ANOVA for repeated measures was performed using JASP software. The outcome of frequentist statistics is limited to the rejection or non-rejection of the null hypothesis based on a *P*-value threshold (usually 0.05). A

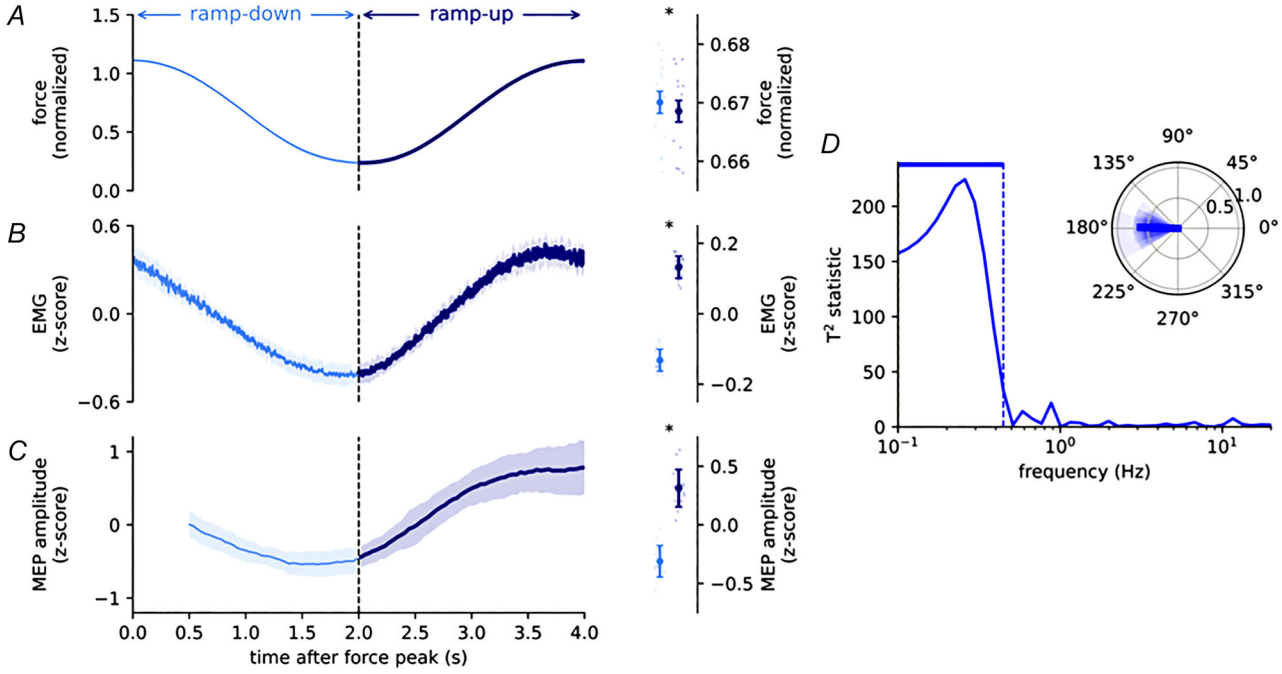


**Figure 3. Modulation of corticospinal excitability at the macroscopic scale**
*A*, average force (produced by the right index finger) time-aligned to the 0.25 Hz force fluctuations (zero-time). *B*, average EMG activity of the right FDI (rectified and *z*-scored) time-aligned to the 0.25 Hz force fluctuations (of the right finger). *C*, average peak-to-peak MEP size (*z*-scored) binned (bin size: 1 s, 43.75 ± 9.56 MEPs per bin, mean ± SD) according to the time of TMS pulse delivery relative to the 0.25 Hz force fluctuations (of the right finger). The shaded areas indicate the mean ± SD. The plots on the right-hand side show individual data and group average data for mean force (*A*), EMG (*B*) and MEP (*C*) during the ramp-up (dark blue) and ramp-down (light blue) phases of the force cycle. Error bars indicate SD. The EMG activity and MEP are significantly larger during the ramp-up phase than during the ramp-down phase. A small yet statistically significant ramp-up *vs*. ramp-down difference is also observed in the force ($t_{13} = -4.694$, $P < 0.001$), though of opposite sign compared to the MEP/EMG modulation, with greater force observed in the ramp-down phase than in the ramp-up phase. *D*, Hotelling's $T^2$-statistic on the $\beta$-coefficients obtained from generalised linear regression analysis; the analysis was performed to test whether sinusoidal functions with frequencies ranging from 0.1 to 20 Hz and with the same phase across participants predict the MEP size (see Methods for more details). The horizontal line indicates significant frequencies (Bonferroni correction for multiple comparisons across frequencies). The polar plot denotes the across-participant distribution (shaded bars) and average value (continuous line) of the mean phase of sinusoidal functions falling within the significant frequency interval. [Colour figure can be viewed at wileyonlinelibrary.com]

non-rejection of the null hypothesis (i.e. $P > 0.05$) does not necessarily indicate that the null hypothesis is true but rather that the available evidence does not provide sufficient support for rejecting the null hypothesis in favour of the alternative. Bayesian statistics, on the other hand, provide the relative strength of the evidence in favour of the alternative hypothesis (in this case, MEP modulation amplitude changes across scales) compared to the null hypothesis (MEP modulation amplitude does not change across scales).

Finally, we normalised the amplitude of MEP modulation and force and EMG oscillations at the 2

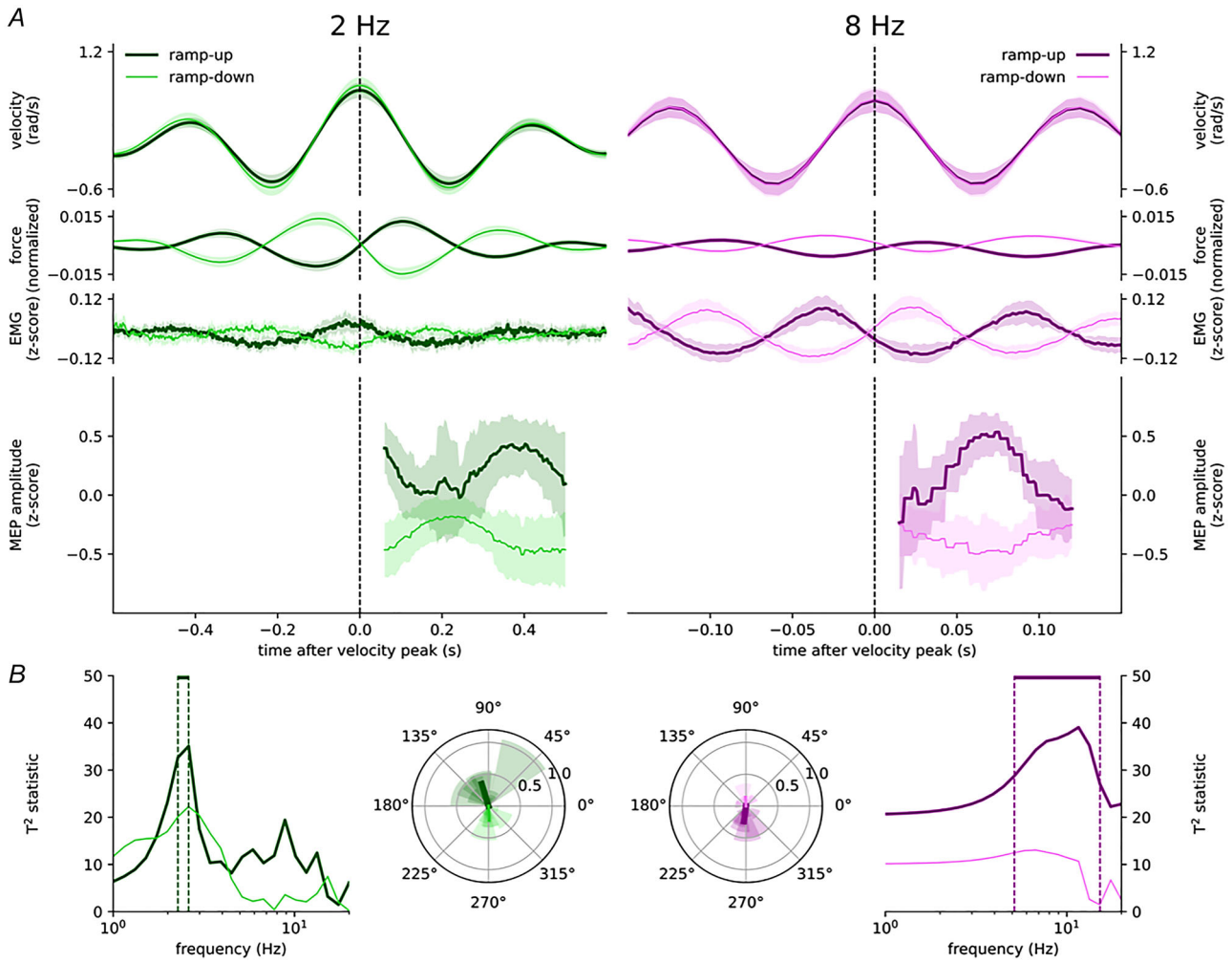


**Figure 4. Modulation of corticospinal excitability at the microscopic scales**
*A*, cursor velocity (first row), force (normalised; second row), EMG (rectified and *z*-scored; third row) averaged across trials and participants. The fourth row shows MEP size averaged across participants after the time-binning procedure and time-aligned to 2 Hz (left-hand panel; bin size: 0.12 s; ramp-up, 19.20 ± 10.25 MEPs/bin; ramp-down, 23.16 ± 12.37 MEPs/bin, mean ± SD) and 8 Hz (right-hand panel; bin size: 0.03; ramp-up, 26.03 ± 18.76 MEPs/bin; ramp-down, 19.40 ± 8.60 MEPs/bin, mean ± SD) velocity peaks for data belonging to the ramp-up (dark lines) and ramp-down (light lines) phase of the cycle. Force and EMG were high-pass filtered (cut-off: 0.5 Hz) to remove the slow, macroscopic 0.25 Hz component. This helps in appreciating the microscopic force/EMG variations and their relationship to the 2 and 8 Hz velocity peaks. Notice that, for biomechanical reasons, force modulations occur a few tens of milliseconds after those in the EMG traces (Cavanagh & Komi, 1979; Inman et al., 1952). The shaded areas represent the mean ± SD. *B*, Hotelling's $T^2$-statistic calculated on the $\beta$-coefficients obtained from generalised linear regression analysis, as done for MEP modulation time-locked to 0.25 Hz force oscillation (see Fig. 3*D*). For the microscopic timescales, the analysis was performed separately for ramp-up and ramp-down data. The horizontal line indicates significant frequencies (ramp-up data only; Bonferroni correction for multiple comparisons across frequencies). As in Fig. 3*D*, the polar plots denote the across-participant distribution (shaded bars) and average value (continuous line) of the mean phase of sinusoidal functions falling within the significant interval. In ramp-down data, no frequency was significant, so the mean phase depicted in the polar plot was calculated in the same interval as ramp-up data. [Colour figure can be viewed at wileyonlinelibrary.com]

and 8 Hz scales to their respective values at the 0.25 Hz scale (separately for ramp-up and ramp-down data). Then, we performed a 3-by-2 ANOVA for repeated measures with 'Motor index' (MEP, force, EMG) and 'Time-scale' (2 Hz, 8 Hz) as within-participant factors. Significant effects were further explored by means of pairwise Bonferroni-corrected paired sample *t* tests.

## Results

Not surprisingly (Hess et al., 1986), corticospinal excitability (Fig. 3*C*) showed fluctuations that closely matched the 4 s force cycle (Fig. 3*A*) and corresponding EMG activity (Fig. 3*B*), with larger/smaller MEPs being associated with larger/smaller force outputs. Specifically, MEP modulation at this timescale was predicted by sinusoidal basis functions having consistent phase across participants for frequencies ranging between 0.1 and 0.4 Hz (Fig. 3*D*), i.e. a frequency interval that was (expectedly) centred on the periodicity instructed by the target rotation rate. Furthermore, both the EMG activity and MEP were larger in the ramp-up phase than in the ramp-down phase of the force cycle (EMG activity: $t_{13} = 15.172$, $P < 0.001$; MEP: $t_{13} = 7.700$, $P < 0.001$; bar plots in Fig. 3*B* and *C*). This finding corroborates previous results showing that changes in corticospinal excitability and EMG activity over a muscle contraction/relaxation cycle occur throughout a hysteresis loop; that is, they are affected not only by the force level but also by the direction of force variation (i.e. ramp-up/ramp-down) (Kimura et al., 2003).

Does corticospinal excitability scale also according to microscopic variations in motor output within the frequency range of submovements and tremor? Figure 4*A* (fourth row) shows that MEPs time aligned to both the 2 Hz (left) and 8 Hz (right) peaks of angular velocity follow a consistent, non-monotonic trend. The direction of this modulation reflects the force variation around the angular velocity peaks, which is opposite in the ramp-up and ramp-down phases of the force cycle. Interestingly, its profile appeared to have a sinusoidal-like shape, especially for the ramp-up data. This was confirmed statistically using the same analytical approach as that used for the macroscopic scale (see Methods). In fact, at both submovements and tremor scales, the modulation of corticospinal excitability was consistent (similar phase across participants) for frequencies ranging from 2.2 to 2.6 Hz and from 5.1 to 15.2 Hz, respectively (Fig. 4*B*). In other words, corticospinal excitability is modulated at submovements and tremor periodicity. No significant modulation was observed at any tested frequency for the ramp-down data.

Angular velocity describes the cursor motion along the direction of target motion but not along all other directions (away from the circular path). Consequently, it does not fully capture the overall motor output generated by the two hands. Thus, we repeated the same analysis using tangential instead of angular velocity. When TMS latencies were calculated based on peaks identified in tangential (as opposed to angular) velocity, the pattern of results was comparable, with significant MEP modulation for ramp-up data at frequencies between 2.0 and 2.6 Hz (2 Hz scale) and between 4.5 and 17.5 Hz (8 Hz scale) and no significant results for ramp-down data.

By task design, the cursor velocity is not 'contaminated' by the macroscopic fluctuation of the force at 0.25 Hz, allowing microscopic fluctuations to be more clearly evidenced. However, the cursor velocity reflects the combined output of the two hands. To ensure that the MEP modulation (microscopic scales) observed following TMS over the left M1 was indeed attributable to the right hand, we repeated the same analysis separately for the (first derivative of) force exerted by the right and left index fingers (i.e. the cursor velocity in the two orthogonal directions of motion controlled independently by the two hands). As expected, when TMS latency was calculated based on right hand force, we obtained significant MEP modulation in the same frequency ranges reported for angular velocity (2 Hz scale: 2.2–2.7 Hz, 8 Hz scale: 4.1–15.2 Hz). In contrast, by expressing TMS latency relative to peaks in the force produced by the left hand, we found no significant MEP modulation at either frequency. This indicates that MEP modulation at the microscopic time-scales reflects the motor commands transmitted to the right finger independently of those sent concurrently to the left finger.

As shown so far, corticospinal excitability undergoes modulations that are multiplexed in frequency and match the periodicities of the motor output at both task-instructed (0.25 Hz) and spontaneous (2/8 Hz) rhythms. Consistent with this finding, correlation coefficients between MEP size and EMG activity time-shifted to account for conduction time from M1 to the muscle (see Methods) were significantly larger than zero (0.25 Hz: $t_{13} = 46.207$, $P < 0.001$; $t_{13} = 13.094$, $P < 0.001$; 2 Hz: $t_{13} = 3.132$, $P = 0.008$; $t_{13} = 2.784$, $P = 0.015$; 8 Hz: $t_{13} = 7.548$, $P < 0.001$; $t_{13} = 3.101$, $P = 0.008$; ramp-up and ramp-down, respectively; one-sample *t* test against zero; Fig. 5*A* and *B*). This indicates that corticospinal excitability shows a positive linear relation with motor output at each timescale, as predicted by well-established previous evidence (Hess et al., 1986).

Surprisingly, however, when we looked across scales, the range of corticospinal excitability modulation did not scale with the associated force/EMG variation (Fig. 6*B*). In fact, the amplitude of force oscillations varied by about

two orders of magnitude from the slowest (i.e. 0.25 Hz) to the fastest (i.e. 8 Hz) time-scale ($P < 0.001$, partial $\eta^2 = 0.999$, both for ramp-up and for ramp-down data; one-way ANOVA for repeated measures; all pairwise tests were statistically significant after Bonferroni correction); the amplitude of the EMG variation was also dramatically reduced (by about five times) from the macroscopic to the microscopic scales ($P < 0.001$, both for ramp-up [partial $\eta^2 = 0.975$] and ramp-down [partial $\eta^2 = 0.972$] data; one-way ANOVA for repeated measures; all pairwise tests were statistically significant after Bonferroni correction except between the 2 Hz and 8 Hz time-scales for ramp-up data). On the other hand, the modulation amplitude of corticospinal excitability (computed as the difference between the maximum and minimum MEP size) appeared quite similar at all scales (ramp-up, 0.25 Hz: 1.368; 2 Hz: 1.137; 8 Hz: 1.239; ramp-down, 0.25 Hz: 0.617; 2 Hz: 0.746; 8 Hz: 0.730; group average data expressed as *z*-scores) with no statistically significant differences (ramp-up, $P = 0.079$; ramp-down, $P = 0.110$; one-way ANOVA for repeated measures). However, the Bayesian ANOVA did not provide strong support in favour of 'evidence of absence' of a difference in the amplitude of MEP modulation across scales (ramp-up, $BF_{10} = 1.099$; ramp-down, $BF_{10} = 0.868$; by convention, evidence of absence requires $BF_{10} < 0.3$). Despite this inconclusive evidence, the current data clearly advocate for scale invariant mapping between corticospinal excitability and motor output. This is particularly evident if we examine the reduction in the amplitude of MEP modulation and oscillations of motor output (both force and EMG) from macro to microscopic scales – i.e. the ratios between the amplitude at the 2 Hz and 8 Hz scales and that at the 0.25 Hz scale. While the reduction across scales was almost negligible for the amplitude of MEP modulation, as shown by ratios being very close to 1 (Fig. 6*C*, left-hand panel; 2 Hz: ramp-up, 0.855 ± 0.272, ramp-down, 1.417 ± 0.650; 8 Hz, ramp-up, 0.930 ± 0.238, ramp-down, 1.323 ± 0.545), it was enormous for the amplitude of both force (Fig. 6*C*, centre panel; 2 Hz: ramp-up, 0.027 ± 0.005, ramp-down, 0.033 ± 0.007; 8 Hz, ramp-up, 0.008 ± 0.003, ramp-down, 0.009 ± 0.003) and EMG (Fig. 6*C*, right-hand panel; 2 Hz: ramp-up, 0.190 ± 0.035, ramp-down, 0.176 ± 0.023; 8 Hz, ramp-up, 0.192 ± 0.088, ramp-down, 0.227 ± 0.074) oscillations, resulting in a statistically significant main effect of 'motor index' ($P < 0.001$, for both ramp-up and ramp-down data; ANOVA for repeated measures). Bonferroni-corrected pairwise comparisons showed that all ratios were larger for MEPs compared to force ($P < 0.001$, for both ramp-up and ramp-down data) and EMG ($P < 0.001$, for both ramp-up and ramp-down data), as well as for EMG compared to force for ramp-up ($P = 0.010$) but not ramp-down data ($P = 0.160$). No other effect reached significance (main effect of 'Timescale', ramp-up, $P = 274$; ramp-down, $P = 0.535$; 'Time-scale' by 'Motor index' interaction: ramp-up, $P = 0.280$; ramp-down, $P = 0.311$).

## Discussion

Movement intermittency and tremor appear as force/velocity fluctuations recurring with ∼2 and 8 Hz periodicity, respectively (Craik, 1947; Elble, 1996; Horsley & Schäfer, 1886; McAuley & Marsden, 2000; Miall et al., 1993; Vallbo & Wessberg, 1993). In most circumstances, they have minimal amplitude and are hardly noticeable. Here, we show that these subtle oscillations engraved in our motor output are coupled

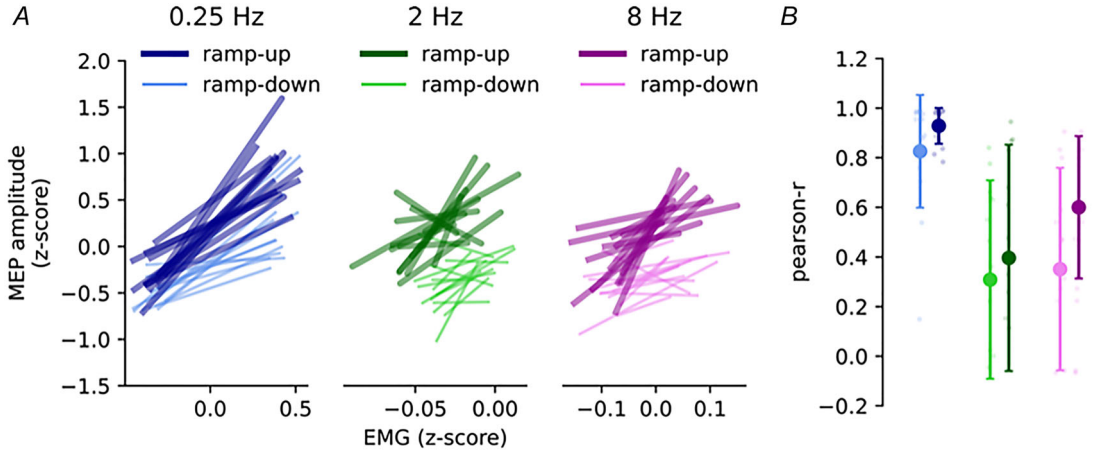


**Figure 5. Corticospinal excitability covaries with the motor output at each time-scale**
*A*, modulation of individual MEPs against EMG activity at 0.25 Hz (left), 2 Hz (middle) and 8 Hz (right) for the ramp-up (dark lines) and ramp-down (light lines) data. Lines show the best-fitting linear functions for the individual data. At each timescale, MEP scales with concurrent EMG activity. *B*, Pearson's correlation coefficient averaged across participants for each timescale and cycle phase. Error bars represent ± SD. [Colour figure can be viewed at wileyonlinelibrary.com]

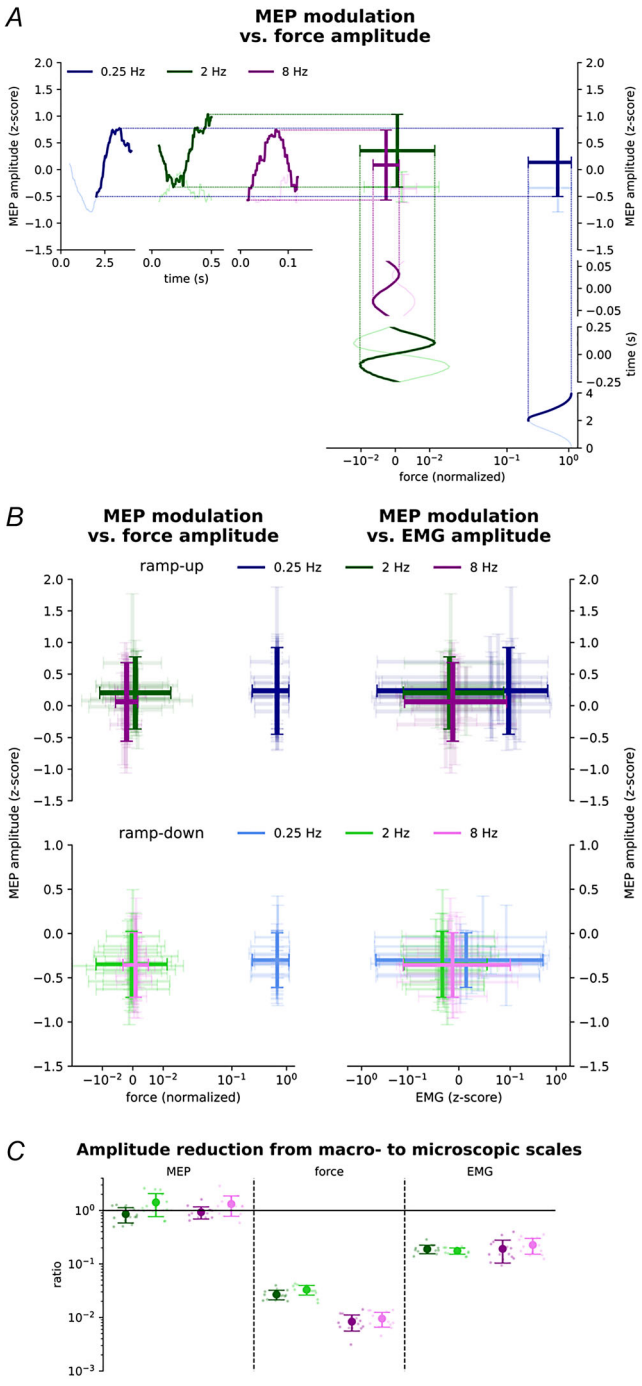


**Figure 6. Scale invariance of corticospinal excitability**
*A*, illustration of the procedure used to estimate the amplitude of MEP modulation and force/EMG oscillations; example data from one participant. Binned MEP size (time-aligned to force/velocity peaks; see Figs 3 and 4, and Methods) is shown in the upper left panel for all time-scales (dark: ramp-up; light: ramp-down). MEP modulation amplitude is calculated as the difference between the maximum and minimum value (binned data) at each time-scale (marked by dotted lines only for ramp-up data for illustrative purposes). The lower right panel shows the force (unfiltered and filtered [0.5 Hz high-pass] for the macro- and microscopic scales, respectively) for time windows corresponding to half an oscillation cycle for the macroscopic scale (i.e. 2 s) and one oscillation cycle for the microscopic scales (i.e. 0.5 and 0.125 s for 2 and 8 Hz, respectively) time-aligned in the same way as the MEP data (i.e. relative to force/velocity peaks; see Figs 3 and 4, and Methods). The oscillation amplitude is calculated as the difference between the maximum and minimum force value at each timescale (marked by dotted lines only for ramp-up data for illustrative purposes). The same procedure was adopted to calculate the amplitude of EMG oscillations. *B*, the mean amplitude of MEP modulation is plotted against the mean amplitude of force (left) and EMG (right) oscillations at the 0.25 Hz (blue), 2 Hz (green) and 8 Hz (violet) scale for the ramp-up (top) and ramp-down (bottom) data. Note that both the force and EMG are plotted on a symmetric logarithmic scale to allow better visualisation of the difference in amplitude between the macro- and microscopic oscillations. The shaded lines represent individual participants while the thick lines represent group average data. *C*, ratios between the amplitude of MEP modulation (left, squares), force oscillations (middle, triangles) and EMG oscillations (right, diamonds) at the 2 Hz (green) and 8 Hz (violet) scales and the respective values at the 0.25 Hz scale. Dark colours denote ramp-up, light colours ramp-down. Light-coloured dots show individual participant data. Error bars indicate ± SD. [Colour figure can be viewed at wileyonlinelibrary.com]

with systematic changes in corticospinal excitability, as indexed by MEP. Most surprisingly, the changes in MEP are comparable in magnitude to those associated with voluntary (task-instructed) force modulations, which are almost two orders of magnitude larger than the 2/8 Hz force fluctuations. In other words, corticospinal excitability shows multiscale fluctuations whose magnitude is almost invariant across scales, varying very little in the face of the associated enormous variation in force outputs.

Corticospinal excitability, as measured via TMS, reflects the combined effect of all inputs to the upper and lower motoneurons at the time of stimulation (Rothwell, 1997), including those from local (Kujirai et al., 1993; Valls-Solé et al., 1992) and long-range cortico-cortical connections (Koch, 2020) as well as reafferent (Tokimura et al., 2000) and subcortical signals (Fisher et al., 2004; Furubayashi et al., 2000; Kühn et al., 2004). This makes the relationship between activity along the corticospinal system and its (TMS-assessed) excitability complex and likely non-linear (Baker et al., 1995; Matthews, 1999). Despite this complexity, corticospinal excitability is generally regarded as a proxy for the descending drive owing to its evident relationship with the motor output (De Noordhout et al., 1992; Hess et al., 1986, 1987). In line with this view, at each time-scale, we observed a positive relationship between corticospinal excitability and the motor output (force/EMG; Fig. 5*A*). This suggests that, at least to some extent, MEP reflects the instantaneous activity flowing along the corticospinal system when TMS is delivered. The hysteretic modulation of corticospinal excitability over a contraction–relaxation cycle – as reported previously (Kimura et al., 2003) and replicated in the present study (see Fig. 3) – has also been interpreted by assuming

a change in the descending inputs to motoneurons. In fact, because of the (passive) mechanical properties of sarcomeres (Herzog et al., 2016) and long-lasting plateau currents occurring in motoneurons (Gorassini et al., 2002), the amount of synaptic drive needed to sustain a certain force output is expected to be lower during the ramp-down phase than during the ramp-up phase (Heckmann et al., 2005), possibly explaining the corresponding modulation of MEP (smaller/larger MEPs in the ramp-down/up phase).

Given the composite nature of corticospinal excitability (reflecting multilevel influences by a plethora of inputs), its relationship with the descending motor drive is not always straightforward. For example, during reaching–grasping movements, neither the amplitude of MEPs mirrors time-varying muscle activity (Johansson et al., 1994; Lemon et al., 1995) nor that of spinal volleys (elicited by TMS) fully matches the discharge of corticospinal neurons (Baker et al., 1995; Bennett & Lemon, 1994; Lemon et al., 1996). Corticospinal excitability is also influenced by a multitude of motor states that do not necessarily entail an overt motor output (e.g. motor preparation, motor imagery, action observation) (Bestmann & Duque, 2016; D'Ausilio et al., 2015; Fadiga et al., 1995, 1998; Rossi et al., 1998). Spontaneous fluctuations in corticospinal excitability are observed even at rest or during steady muscle contraction. These fluctuations have been related to ongoing oscillatory brain activity, especially in the alpha- and beta-band (Bergmann et al., 2019; Karabanov et al., 2021; Keil et al., 2014; Madsen et al., 2019; Mäki & Ilmoniemi, 2010; Ogata et al., 2019; Sauseng et al., 2009; Berger et al., 2014; Schaworonkow et al., 2018, 2019; Schulz et al., 2014; Thies et al., 2018; Wischnewski et al., 2022; Zarkowski et al., 2006). Similarly, fluctuations in EMG activity recorded during steady-state contraction over a rather wide spectral range (∼5–60 Hz) have a clear relationship with MEP size (Mitchell et al., 2007; van Elswijk et al., 2010).

Here, we investigated corticospinal excitability modulations locked to well-known overt oscillations (i.e. intermittency and tremor) that are naturally embedded in motor output during dynamic motor control. Discontinuities at ∼2 Hz and 8 Hz often coexist in the output (Vallbo & Wessberg, 1993), but their origin (peripheral *vs*. central) and significance (functional role *vs*. neuromotor noise) are still debated. In fact, some accounts posit that these discontinuities originate peripherally as a by-product of biomechanical properties (Dounskaia et al., 2005; Vernooij et al., 2013), whereas others suggest that they reflect central neural activity, at least to a certain extent (Dipietro et al., 2014; Gross et al., 2002; Hall et al., 2014; Jerbi et al., 2007; Mehta et al., 2014; Pereira et al., 2017; Rouse et al., 2022; Susilaradeya et al., 2019; Tomassini et al., 2020; Williams et al., 2009). The latter hypothesis is mostly supported by studies quantifying the coupling (e.g. phase synchronisation) between cortical/subcortical activities and the motor output (kinematics/force/EMG), and possibly inferring (analytically) its directional selectivity (Gross et al., 2002; Tomassini et al., 2020; Witham et al., 2011; Yang et al., 2018). In many cases, this set of evidence has pointed to a non-negligible, sometimes primary, contribution of (re)afferent activity (Bourguignon et al., 2019; Oya et al., 2020; Williams et al., 2009), calling into question the exclusive influence of descending signals on peripheral oscillations. Similarly, afferent signals are known to play a role in modulating corticospinal excitability (e.g. see Tokimura et al., 2000). Yet, irrespective of the efferent/(re)afferent origin, the present study shows that corticospinal excitability modulates according to fluctuations in motor output in a non-trivial manner, that is, independently of their actual amplitude scaling.

In fact, the most remarkable aspect of the present findings is that the range of variation in corticospinal excitability remains very similar across the three (time) scales (i.e. 0.25, 2 and 8 Hz). In contrast, the amplitude of force fluctuations varies by about two orders of magnitude from the 0.25- to the 8-Hz scale. Likewise, EMG oscillation amplitude is largely reduced (by about five times) from the macroscopic to the microscopic scale. This high non-linearity suggests that corticospinal excitability indexes a relatively abstract level of motor encoding that reflects the temporal organisation of corticospinal communication at multiple time-scales, but not the direct encoding of actual force (or muscle activity). Whether the descending corticospinal drive itself maintains a similar non-linear relationship with the motor output remains to be determined (as we have argued above, TMS-derived measures of corticospinal excitability cannot be taken as a direct proxy of corticospinal activity). Under this hypothesis, a rescaling operation would be required before corticospinal signals are transmitted to the muscles. This could be analogous to a low-pass filtering operation: the descending cortical drive could contain oscillations with the same amplitude at all relevant time-scales (i.e. 0.25, 2, and 8 Hz); this signal would then be low-pass filtered downstream, keeping the amplitude of the 0.25 Hz motor drive unchanged, while attenuating the higher frequency components at 2 and 8 Hz, as shown in the overt motor output. Such an encoding scheme might increase the precision of the control signals at microscopic (time)scales. More specifically, for the same reason we downshift gears in a car, the smaller the force variations to be controlled, the greater the depth of encoding that can be achieved using the same neural signals. At the same time, the purported filtering mechanism would dampen high-frequency components in the neural drive to prevent their massive spilling over into the motor output which might be detrimental to motor performance.

Some hypotheses can be put forth regarding how such putative rescaling might actually be implemented. The viscoelastic properties of muscles and the relatively sluggish electromechanical coupling between motor unit activity and force generation act *de facto* as low-pass filters (Bawa & Stein, 1976; Mannard & Stein, 1973). Although such attenuation mainly affects higher frequencies (>15 Hz; Burke, 2011), it may still exert a limited effect at 8 Hz. This is in line with the observation that the 8 Hz and 2 Hz oscillations display comparable amplitudes at the muscle level (i.e. in the EMG activity), while for the force, the 8 Hz oscillations are smaller than the 2 Hz oscillations. However, biomechanical attenuation certainly cannot account for the huge drop in the force/EMG amplitude modulation from the macro- to microscopic scales, which is yet accompanied by comparable modulations of corticospinal excitability. Thus, substantial attenuation should originate from extrapyramidal descending tracts and/or directly within spinal circuitries. In this regard, 8–10 Hz activity in spinal interneurons (and even at lower frequencies to a certain extent) has been shown to be out-of-phase with cortical (M1) activity. This may produce phase-cancellation of the oscillatory drive at the motoneuron level, with a consequent reduction in tremor amplitude (Williams et al., 2010). Interestingly, a similar antiphase relationship between spinal and cortical motor activity is observed in response to peripheral nerve stimulation, pointing to the possible involvement of feedback-based mechanisms in regulating oscillations in the motor output (Koželj & Baker, 2014; but see also Galán & Baker, 2015).

Sensory feedback, particularly visual feedback, is believed to largely sculpt the microstructure of movement also over a slower time-scale, such as that characterising intermittency at ∼2 Hz (Miall, 1996; Miall et al., 1993; Susilaradeya et al., 2019; Vallbo & Wessberg, 1993). Classical and recent work has documented that movement discontinuities in the 2 Hz range are systematically affected by visual feedback manipulation (Miall, 1996; Susilaradeya et al., 2019; Miall et al., 1993; Vallbo & Wessberg, 1993; but see also Doeringer & Hogan, 1998). Fluctuations in movement velocity around 2 Hz also become synchronised between two (visually) interacting partners, suggesting that they might play a role in motor coordination (Tomassini et al., 2022; Nazzaro et al., 2023). Indeed, it has been suggested that 2 Hz intermittency may substantially reflect the closing of a sensorimotor loop. More generally, accumulating evidence supports an intrinsic coupling between motor and sensory rhythms. For example, ongoing fluctuations in visual activity and perceptual sensitivity have been shown to be time-locked to hand movements (Benedetto et al., 2016, 2021; Nakayama & Motoyoshi, 2019; Tomassini et al., 2015, 2017; Zhang et al., 2019) and to be phase reset by exogenous activation of the somatomotor hand system (Tomassini & D'Ausilio, 2018). Furthermore, during continuous isometric force control, visual detection is enhanced at moments when alpha-band corticospinal coherence is greater (Tomassini et al., 2020). Taken together, these findings suggest that oscillation-based mechanisms may contribute to synchronise sensory sampling/processing with the issuing of motor commands (Benedetto et al., 2020; Schroeder et al., 2010).

In conclusion, our results demonstrate that sustained motor output contains visible traces of oscillatory signals that are multiplexed in frequency and coupled with scale-invariant changes in corticospinal excitability. This might reflect a specific control strategy endowing the sensorimotor system with greater flexibility and temporal precision. Whether these results generalise to other types of motor tasks (e.g. isometric *vs*. non-isometric motor output, discrete *vs*. continuous motor control, dominant *vs*. non-dominant hand) should be addressed in future research. Importantly, gaining insight into how the sensorimotor system dynamically sculpts motor output across multiple (time) scales could provide valuable information for understanding brain disorders characterised by visible alterations in the physiological architecture of movements (e.g. the different tremors observed in cerebellar, Parkinson's or psychiatric populations) (Elble, 2013; Raethjen & Deuschl, 2009; Zeuner & Deuschl, 2012). Future studies could investigate whether the dynamics and scale invariance of corticospinal excitability represent potential biomarkers of conditions associated with dysfunction of the cortico-subcortical networks underlying the multiscale organisation of movement (e.g. cortico-cerebellar and cortico-basal ganglia circuits) or could possibly index alterations in the metabolism and distribution of specific neurotransmitters.

## References

Baker, S. N., Olivier, E., & Lemon, R. N. (1995). Task-related variation in corticospinal output evoked by transcranial magnetic stimulation in the macaque monkey. *The Journal of Physiology*, **488**(3), 795–801.

Bawa, P., & Stein, R. B. (1976). Frequency response of human soleus muscle. *Journal of Neurophysiology*, **39**(4), 788–793.

Benedetto, A., Binda, P., Costagli, M., Tosetti, M., & Morrone, M. C. (2021). Predictive visuo-motor communication through neural oscillations. *Current Biology*, **31**(15), 3401–3408.e4.e4.

Benedetto, A., Morrone, M. C., & Tomassini, A. (2020). The common rhythm of action and perception. *Journal of Cognitive Neuroscience*, **32**(2), 187–200.

Benedetto, A., Spinelli, D., & Morrone, M. C. (2016). Rhythmic modulation of visual contrast discrimination triggered by action. *Proceedings of the Royal Society*, **283**, 20160692.

Bennett, K. M., & Lemon, R. N. (1994). The influence of single monkey cortico-motoneuronal cells at different levels of activity in target muscles. *The Journal of Physiology*, **477**(2), 291–307.

Berger, B., Minarik, T., Liuzzi, G., Hummel, F. C., & Sauseng, P. (2014). EEG oscillatory phase-dependent markers of corticospinal excitability in the resting brain. *BioMed Research International*, **2014**, 1.

Bergmann, T. O., Lieb, A., Zrenner, C., & Ziemann, U. (2019). Pulsed facilitation of corticospinal excitability by the sensorimotor $\mu$-alpha rhythm. *Journal of Neuroscience*, **39**(50), 10034–10043.

Bernhard, C. G., Bohm, E., & Petersén, I. (1953). New investigations on the pyramidal system in Macaca mulatta. *Experientia*, **9**(3), 111–112.

Bestmann, S., & Duque, J. (2016). Transcranial magnetic stimulation: Decomposing the processes underlying action preparation. *The Neuroscientist*, **22**, 392–405.

Bourguignon, M., Jousmäki, V., Dalal, S. S., Jerbi, K., & De Tiège, X. (2019). Coupling between human brain activity and body movements: Insights from non-invasive electromagnetic recordings. *Neuroimage*, **203**, 116177.

Brainard, D. H. (1997). The Psychophysics Toolbox. *Spatial Vision*, **10**(4), 433–436.

Burke, R. E. (2011). Motor units: Anatomy, physiology, and functional organization. In *Comprehensive physiology*, pp. 345–422. John Wiley & Sons, Ltd. https://onlinelibrary.wiley.com/doi/abs/10.1002/cphy.cp010210

Cavanagh, P. R., & Komi, P. V. (1979). Electromechanical delay in human skeletal muscle under concentric and eccentric contractions. *European Journal of Applied Physiology*, **42**(3), 159–163.

Craik, K. J. W. (1947). Theory of the human operator in control systems; the operator as an engineering system. *British Journal of Psychology. General Section*, **38**(2), 56–61.

D'ausilio, A., Bartoli, E., & Maffongelli, L. (2015). Grasping synergies: A motor-control approach to the mirror neuron mechanism. *Physics of Life Reviews*, **12**, 91–103.

De Noordhout, A. M., Pepin, J. L., Gerard, P., & Delwaide, P. J. (1992). Facilitation of responses to motor cortex stimulation: Effects of isometric voluntary contraction. *Annals of Neurology*, **32**(3), 365–370.

Lazzaro, V. D.i, Ziemann, U., & Lemon, R. N. (2008). State of the art: Physiology of transcranial motor cortex stimulation. *Brain Stimulation*, **1**(4), 345–362.

Dipietro, L., Poizner, H., & Krebs, H. I. (2014). Spatiotemporal dynamics of online motor correction processing revealed by high-density electroencephalography. *Journal of Cognitive Neuroscience*, **26**(9), 1966–1980.

Doeringer, J. A., & Hogan, N. (1998). Intermittency in preplanned elbow movements persists in the absence of visual feedback. *Journal of Neurophysiology*, **80**(4), 1787–1799.

Dounskaia, N., Wisleder, D., & Johnson, T. (2005). Influence of biomechanical factors on substructure of pointing movements. *Experimental Brain Research*, **164**(4), 505–516.

Elble, R. J. (1996). Central mechanisms of tremor. *Journal of Clinical Neurophysiology*, **13**(2), 133–144.

Elble, R. J. (2013). Tremor disorders. *Current Opinion in Neurology*, **26**(4), 413–419.

Van Elswijk, G., Maij, F., Schoffelen, J.-M., Overeem, S., Stegeman, D. F., & Fries, P. (2010). Corticospinal beta-band synchronization entails rhythmic gain modulation. *Journal of Neuroscience*, **30**(12), 4481–4488.

Fadiga, L., Buccino, G., Craighero, L., Fogassi, L., Gallese, V., & Pavesi, G. (1998). Corticospinal excitability is specifically modulated by motor imagery: A magnetic stimulation study. *Neuropsychologia*, **37**(2), 147–158.

Fadiga, L., Fogassi, L., Pavesi, G., & Rizzolatti, G. (1995). Motor facilitation during action observation: A magnetic stimulation study. *Journal of Neurophysiology*, **73**(6), 2608–2611.

Fisher, R. J., Sharott, A., KüHn, A. A., & Brown, P. (2004). Effects of combined cortical and acoustic stimuli on muscle activity. *Experimental Brain Research*, **157**(1), 1–9.

Fregosi, M., Contestabile, A., Hamadjida, A., & Rouiller, E. M. (2017). Corticobulbar projections from distinct motor cortical areas to the reticular formation in macaque monkeys. *European Journal of Neuroscience*, **45**(11), 1379–1395.

Furubayashi, T., Ugawa, Y., Terao, Y., Hanajima, R., Sakai, K., Machii, K., Mochizuki, H., Shiio, Y., Uesugi, H., Enomoto, H., & Kanazawa, I. (2000). The human hand motor area is transiently suppressed by an unexpected auditory stimulus. *Clinical Neurophysiology*, **111**(1), 178–183.

Galán, F., & Baker, S. N. (2015). Pre-synaptic inhibition of afferent feedback in the macaque spinal cord does not modulate with cycles of peripheral oscillations around 10 Hz. *Frontiers in Neural Circuits*, **9**, 76.

Gorassini, M., Yang, J. F., Siu, M., & Bennett, D. J. (2002). Intrinsic activation of human motoneurons: possible contribution to motor unit excitation. *Journal of Neurophysiology*, **87**(4), 1850–1858.

Gross, J., Timmermann, L., Kujala, J., Dirks, M., Schmitz, F., Salmelin, R., & Schnitzler, A. (2002). The neural basis of intermittent motor control in humans. *Proceedings of the National Academy of Sciences, USA*, **99**(4), 2299–2302.

Hall, T. M., De Carvalho, F., & Jackson, A. (2014). A common structure underlies low-frequency cortical dynamics in movement, sleep, and sedation. *Neuron*, **83**(5), 1185–1199.

Heckman, C. J., Gorassini, M. A., & Bennett, D. J. (2005). Persistent inward currents in motoneuron dendrites: implications for motor output. *Muscle & Nerve*, **31**(2), 135–156.

Herzog, W., Schappacher, G., DuVall, M., Leonard, T. R., & Herzog, J. A. (2016). Residual force enhancement following eccentric contractions: A new mechanism involving titin. *Physiology*, **31**, 300–312.

Hess, C. W., Mills, K. R., & Murray, N. M. (1987). Responses in small hand muscles from magnetic stimulation of the human brain. *The Journal of Physiology*, **388**(1), 397.

Hess, C. W., Mills, K. R., & Murray, N. M. F. (1986). Magnetic stimulation of the human brain: Facilitation of motor responses by voluntary contraction of ipsilateral and contralateral muscles with additional observations on an amputee. *Neuroscience Letters*, **71**(2), 235–240.

Horsley, V., & Schäfer, E. A. (1886). Experiments on the character of the muscular contractions which are evoked by excitation of the various parts of the motor tract. *The Journal of Physiology*, **7**(2), 96–110.

Inman, V. T., Ralston, H. J., De CM Saunders, J. B., Bertram Feinstein, M. B., & Wright, E. W. (1952). Relation of human electromyogram to muscular tension. *Electroencephalography and Clinical Neurophysiology*, **4**(2), 187–194.

Jerbi, K., Lachaux, J.-P., N′Diaye, K., Pantazis, D., Leahy, R. M., Garnero, L., & Baillet, S. (2007). Coherent neural representation of hand speed in humans revealed by MEG imaging. *Proceedings of the National Academy of Sciences, USA*, **104**(18), 7676–7681.

Johansson, R. S., Lemon, R. N., & Westling, G. (1994). Time-varying enhancement of human cortical excitability mediated by cutaneous inputs during precision grip. *The Journal of Physiology*, **481**(Pt 3), 761–775.

Karabanov, A. N., Madsen, K. H., Krohne, L. G., & Siebner, H. R. (2021). Does pericentral mu-rhythm "power" corticomotor excitability? – A matter of EEG perspective. *Brain Stimulation*, **14**(3), 713–722.

Keil, J., Timm, J., Sanmiguel, I., Schulz, H., Obleser, J., & Schönwiesner, M. (2014). Cortical brain states and corticospinal synchronization influence TMS-evoked motor potentials. *Journal of Neurophysiology*, **111**(3), 513–519.

Keizer, K., & Kuypers, H. G. J. M. (1989). Distribution of corticospinal neurons with collaterals to the lower brain stem reticular formation in monkey (Macaca fascicularis). *Experimental Brain Research*, **74**(2), 311–318.

Keysers, C., Gazzola, V., & Wagenmakers, E.-J. (2020). Using Bayes factor hypothesis testing in neuroscience to establish evidence of absence. *Nature Neuroscience*, **23**(7), 788–799.

Kimura, T., Yamanaka, K., Nozaki, D., Nakazawa, K., Miyoshi, T., Akai, M., & Ohtsuki, T. (2003). Hysteresis in corticospinal excitability during gradual muscle contraction and relaxation in humans. *Experimental Brain Research*, **152**(1), 123–132.

Koch, G. (2020). Cortico-cortical connectivity: The road from basic neurophysiological interactions to therapeutic applications. *Experimental Brain Research*, **238**(7–8), 1677–1684.

Koželj, S., & Baker, S. N. (2014). Different phase delays of peripheral input to primate motor cortex and spinal cord promote cancellation at physiological tremor frequencies. *Journal of Neurophysiology*, **111**(10), 2001–2016.

Kühn, A., Sharott, A., Trottenberg, T., Kupsch, A., & Brown, P. (2004). Motor cortex inhibition induced by acoustic stimulation. *Experimental Brain Research*, **158**(1), 120–124.

Kujirai, T., Caramia, M. D., Rothwell, J. C., Day, B. L., Thompson, P. D., Ferbert, A., Wroe, S., Asselman, P., & Marsden, C. D. (1993). Corticocortical inhibition in human motor cortex. *The Journal of Physiology*, **471**(1), 501–519.

Kuypers, H. (1964). The descending pathways to the spinal cord, their anatomy and function. In *Progress in brain research*, ed. Eccles JC & Schadé JP, Organization of the Spinal Cord, pp. 178–202. Elsevier. https://www.sciencedirect.com/science/article/pii/S0079612308640480

Lemon, R. N. (2008). Descending pathways in motor control. *Annual Review of Neuroscience*, **31**(1), 195–218.

Lemon, R.n, Johansson, R.s, & Westling, G. (1995). Corticospinal control during reach, grasp, and precision lift in man. *Journal of Neuroscience*, **15**(9), 6145–6156.

Lemon, R. N., Johansson, R. S., & Westling, G. (1996). Modulation of corticospinal influence over hand muscles during gripping tasks in man and monkey. *Canadian Journal of Physiology and Pharmacology*, **74**(4), 547–558.

Madsen, K. H., Karabanov, A. N., Krohne, L. G., Safeldt, M. G., Tomasevic, L., & Siebner, H. R. (2019). No trace of phase: Corticomotor excitability is not tuned by phase of pericentral mu-rhythm. *Brain Stimulation*, **12**(5), 1261–1270.

Mäki, H., & Ilmoniemi, R. J. (2010). EEG oscillations and magnetically evoked motor potentials reflect motor system excitability in overlapping neuronal populations. *Clinical Neurophysiology*, **121**(4), 492–501.

Mannard, A., & Stein, R. B. (1973). Determination of the frequency response of isometric soleus muscle in the cat using random nerve stimulation. *The Journal of Physiology*, **229**(2), 275–296.

Marshall, J., & Walsh, E. G. (1956). Physiological tremor. *Journal of Neurology, Neurosurgery, and Psychiatry*, **19**(4), 260–267.

Matthews, P. B. C. (1999). The effect of firing on the excitability of a model motoneurone and its implications for cortical stimulation. *The Journal of Physiology*, **518**(3), 867–882.

Mcauley, J. H. (2000). Physiological and pathological tremors and rhythmic central motor control. *Brain*, **123**(8), 1545–1567.

Mehta, A. R., Brittain, J.-S., & Brown, P. (2014). The selective influence of rhythmic cortical versus cerebellar transcranial stimulation on human physiological tremor. *Journal of Neuroscience*, **34**(22), 7501–7508.

Miall, R. C. (1996). Task-dependent changes in visual feedback control: A frequency analysis of human manual tracking. *Journal of Motor Behavior*, **28**(2), 125–135.

Miall, R. C., Weir, D. J., & Stein, J. F. (1986). Manual tracking of visual targets by trained monkeys. *Behavioural Brain Research*, **20**(2), 185–201.

Miall, R. C., Weir, D. J., & Stein, J. F. (1993). Intermittency in human manual tracking tasks. *Journal of Motor Behavior*, **25**(1), 53–63.

Mitchell, W. K., Baker, M. R., & Baker, S. N. (2007). Muscle responses to transcranial stimulation in man depend on background oscillatory activity. *The Journal of Physiology*, **583**(2), 567–579.

Nakayama, R., & Motoyoshi, I. (2019). Attention periodically binds visual features as single events depending on neural oscillations phase-locked to action. *Journal of Neuroscience*, **39**(21), 4153–4161.

Nazzaro, G., Emanuele, M., Laroche, J., Esposto, C., Fadiga, L. D', Ausilio, A., & Tomassini, A. (2023). The microstructure of intra- and interpersonal coordination. *Proceedings of the Royal Society B: Biological Sciences*, **290**(2011), 20231576.

Ogata, K., Nakazono, H., Uehara, T., & Tobimatsu, S. (2019). Prestimulus cortical EEG oscillations can predict the excitability of the primary motor cortex. *Brain Stimulation*, **12**(6), 1508–1516.

Oya, T., Takei, T., & Seki, K. (2020). Distinct sensorimotor feedback loops for dynamic and static control of primate precision grip. *Communications Biology*, **3**(1), 156.

Pelli, D. G. (1997). The VideoToolbox software for visual psychophysics: Transforming numbers into movies. *Spatial Vision*, **10**(4), 437–442.

Pereira, M., Sobolewski, A., & Millán, J. D. R. (2017). Action monitoring cortical activity coupled to submovements. *eNeuro*, **4**(5), ENEURO.0241–17.2017.

Raethjen, J., & Deuschl, G. (2009). Tremor. *Current Opinion in Neurology*, **22**(4), 400–405.

Rossi, S., Hallett, M., Rossini, P. M., & Pascual-Leone, A. (2009). Safety, ethical considerations, and application guidelines for the use of transcranial magnetic stimulation in clinical practice and research. *Clinical Neurophysiology*, **120**(12), 2008–2039.

Rossi, S., Pasqualetti, P., Tecchio, F., Pauri, F., & Rossini, P. M. (1998). Corticospinal excitability modulation during mental simulation of wrist movements in human subjects. *Neuroscience Letters*, **243**(1–3), 147–151.

Rothwell, J. C. (1997). Techniques and mechanisms of action of transcranial stimulation of the human motor cortex. *Journal of Neuroscience Methods*, **74**(2), 113–122.

Rouse, A. G., Schieber, M. H., & Sarma, S. V. (2022). Cyclic, condition-independent activity in primary motor cortex predicts corrective movement behavior. *eNeuro*, **9**(2), ENEURO.0354-21.2022.

Sauseng, P., Klimesch, W., Gerloff, C., & Hummel, F. C. (2009). Spontaneous locally restricted EEG alpha activity determines cortical excitability in the motor cortex. *Neuropsychologia*, **47**(1), 284–288.

Schaworonkow, N., Caldana Gordon, P., Belardinelli, P., Ziemann, U., Bergmann, T. O., & Zrenner, C. (2018). $\mu$-rhythm extracted with personalized EEG filters correlates with corticospinal excitability in real-time phase-triggered EEG-TMS. *Frontiers in Neuroscience*, **12**, 954.

Schaworonkow, N., Triesch, J., Ziemann, U., & Zrenner, C. (2019). EEG-triggered TMS reveals stronger brain state-dependent modulation of motor evoked potentials at weaker stimulation intensities. *Brain Stimulation*, **12**(1), 110–118.

Scheuer, C., Boot, E., Carse, N., Clardy, A., Gallagher, J., Heck, S., Marron, S., Martinez-Alvarez, L., Masarykova, D., Mcmillan, P., Murphy, F., Steel, E., Ekdom, H. V., & Vecchione, H. (2007). What's new in psychtoolbox-3 ed. Balint G, Antala B, Carty C, Mabieme J-MA, Amar IB & Kaplanova A. *Perception*, **36**, 1–16.

Schroeder, C. E., Wilson, D. A., Radman, T., Scharfman, H., & Lakatos, P. (2010). Dynamics of active sensing and perceptual selection. *Current Opinion in Neurobiology*, **20**(2), 172–176.

Schulz, H., Ubelacker, T., Keil, J., Muller, N., & Weisz, N. (2014). Now I am Ready—Now I am not: The influence of Pre-TMS oscillations and corticomuscular coherence on motor-evoked potentials. *Cerebral Cortex*, **24**(7), 1708–1719.

Sherrington, C. S. (1904). *Correlation of reflexes and the principle of the common path*. British Association Reports.

Susilaradeya, D., Xu, W., Hall, T. M., Galán, F., Alter, K., & Jackson, A. (2019). Extrinsic and intrinsic dynamics in movement intermittency. *eLife*, **8**, e40145.

Thies, M., Zrenner, C., Ziemann, U., & Bergmann, T. O. (2018). Sensorimotor mu-alpha power is positively related to corticospinal excitability. *Brain Stimulation*, **11**(5), 1119–1122.

Tokimura, H., Di Lazzaro, V., Tokimura, Y., Oliviero, A., Profice, P., Insola, A., Mazzone, P., Tonali, P., & Rothwell, J. C. (2000). Short latency inhibition of human hand motor cortex by somatosensory input from the hand. *The Journal of Physiology*, **523**(2), 503–513.

Tomassini, A., Ambrogioni, L., Medendorp, W. P., & Maris, E. (2017). Theta oscillations locked to intended actions rhythmically modulate perception. *eLife*, **6**, e25618.

Tomassini, A., & D'ausilio, A. (2018). Passive sensorimotor stimulation triggers long lasting alpha-band fluctuations in visual perception. *Journal of Neurophysiology*, **119**(2), 380–388.

Tomassini, A., Laroche, J., Emanuele, M., Nazzaro, G., Petrone, N., Fadiga, L., & D'ausilio, A. (2022). Interpersonal synchronization of movement intermittency. *Iscience*, **25**(4), 104096.

Tomassini, A., Maris, E., Hilt, P., Fadiga, L., & D'ausilio, A. (2020). Visual detection is locked to the internal dynamics of cortico-motor control. *PLoS Biology*, **18**(10), e3000898.

Tomassini, A., Spinelli, D., Jacono, M., Sandini, G., & Morrone, M. C. (2015). Rhythmic oscillations of visual contrast sensitivity synchronized with action. *Journal of Neuroscience*, **35**(18), 7019–7029.

Vallbo, A. B., & Wessberg, J. (1993). Organization of motor output in slow finger movements in man. *The Journal of Physiology*, **469**(1), 673–691.

Valls-Solé, J., Pascual-Leone, A., Wassermann, E. M., & Hallett, M. (1992). Human motor evoked responses to paired transcranial magnetic stimuli. *Electroencephalography and Clinical Neurophysiology/Evoked Potentials Section*, **85**(6), 355–364.

Vernooij, C. A., Reynolds, R. F., & Lakie, M. (2013). A dominant role for mechanical resonance in physiological finger tremor revealed by selective minimization of voluntary drive and movement. *Journal of Neurophysiology*, **109**(9), 2317–2326.

Virtanen, P., Gommers, R., Oliphant, T. E., Haberland, M., Reddy, T., Cournapeau, D., Burovski, E., Peterson, P., Weckesser, W., Bright, J., Van Der Walt, S. J., Brett, M., Wilson, J., Millman, K. J., Mayorov, N., Nelson, A. R. J., Jones, E., Kern, R., Larson, E., …, Vázquez-Baeza, Y. (2020). SciPy 1.0: Fundamental algorithms for scientific computing in Python. *Nature Methods*, **17**(3), 261–272.

Williams, E. R., Soteropoulos, D. S., & Baker, S. N. (2009). Coherence between motor cortical activity and peripheral discontinuities during slow finger movements. *Journal of Neurophysiology*, **102**(2), 1296–1309.

Williams, E. R., Soteropoulos, D. S., & Baker, S. N. (2010). Spinal interneuron circuits reduce approximately 10-Hz movement discontinuities by phase cancellation. *Proceedings of the National Academy of Sciences, USA*, **107**(24), 11098–11103.

Wischnewski, M., Haigh, Z. J., Shirinpour, S., Alekseichuk, I., & Opitz, A. (2022). The phase of sensorimotor mu and beta oscillations has the opposite effect on corticospinal excitability. *Brain Stimulation*, **15**(5), 1093–1100.

Witham, C. L., Riddle, C. N., Baker, M. R., & Baker, S. N. (2011). Contributions of descending and ascending pathways to corticomuscular coherence in humans. *The Journal of Physiology*, **589**(15), 3789–3800.

Woodworth, R. S. (1899). Accuracy of voluntary movement. *The Psychological Review: Monograph Supplements*, **3**(3), i–114.

Yang, Y., Dewald, J. P. A., Van Der Helm, F. C. T., & Schouten, A. C. (2018). Unveiling neural coupling within the sensorimotor system: directionality and nonlinearity. *European Journal of Neuroscience*, **48**(7), 2407–2415.

Zarkowski, P., Shin, C. J., Dang, T., Russo, J., & Avery, D. (2006). EEG and the variance of motor evoked potential amplitude. *Clinical EEG and Neuroscience*, **37**(3), 247–251.

Zeuner, K. E., & Deuschl, G. (2012). An update on tremors. *Current Opinion in Neurology*, **25**(4), 475–482.

Zhang, H., Morrone, M. C., & Alais, D. (2019). Behavioural oscillations in visual orientation discrimination reveal distinct modulation rates for both sensitivity and response bias. *Scientific Reports*, **9**(1), 1115.

## Additional information

### Data availability statement

Data from this study will be made available on a public repository upon acceptance for publication.

### Competing interests

The authors declare they have no competing interests.

### Author contributions

M.E.: conceptualisation; investigation; software; formal analysis; visualisation; writing – original draft; writing-review and editing. A.D.: conceptualisation; supervision; writing-review and editing; funding acquisition. G.K.: writing-review and editing. L.F.: writing-review and editing; funding acquisition. A.T.: conceptualisation; supervision; methodology; software; writing-review and editing; funding acquisition. All authors read and approved the final version of the manuscript and agree to be accountable for all aspects of the work in ensuring that questions related to the accuracy or integrity of any part of the work are appropriately investigated and resolved. All persons designated as authors qualify for authorship, and all those who qualify for authorship are listed.

### Funding

This work has been supported by the BIAL Foundation – Grant for Scientific Research 2020 to A.T. (Grant No.246/20), by Ministero della Salute, Ricerca Finalizzata 2016 – Giovani Ricercatori (GR-2016-0 236 1008) and Ministero della Salute, Ricerca Finalizzata 2018 - Giovani Ricercatori (GR-2018-12 366 027) to A.D., by Grant PRIN 2020 to L.F. and by the European Union H2020 - EnTimeMent (FETPROACT-824 160) to L.F. The funders had no role in study design, data collection and analysis, decision to publish, or preparation of the manuscript.

### Acknowledgements

The authors would like to thank Stuart Baker and Giacomo Novembre for reading an early version of the manuscript and providing valuable comments and suggestions.

### Keywords

corticospinal excitability, motor control, physiological tremor, submovements, transcranial magnetic stimulation

## Supporting information

Additional supporting information can be found online in the Supporting Information section at the end of the HTML view of the article. Supporting information files available:

**Peer Review History**